ChemComm
Chemical Communications

Accepted Manuscript

This article can be cited before page numbers have been issued, to do this please use: D. Biswakarma, N. Dey and S. Bhattacharya, *Chem. Commun.*, 2020, DOI: 10.1039/D0CC00839G.

ROYAL SOCIETY OF CHEMISTRY

rsc.li/chemcomm

View Article Online
DOI: 10.1039/D0CC00839G

COMMUNICATION

A Thermo-responsive Supramolecular Hydrogel that Senses Cholera Toxin via Color-Changing Response

Received 00th January 20xx,
Accepted 00th January 20xx

DOI: 10.1039/x0xx00000x

Dipen Biswakarma,[a] Nilanjan Dey [a] and Santanu Bhattacharya *[a,b]

A Pyrene-based amphiphile with C4-alkanoyl spacer and lactose (PyLac) self-assembles in the aqueous media to form an injectable hydrogel. It shows preferential binding with Cholera Toxin (CT) via its terminal galactose residue, and hence can be employed for the selective detection of CT via color-changing response.

Hydrogels belong to the class of functional soft materials due to their easily tuneable optoelectronic properties and large structural diversity. Particularly, hydrogels formed by the self- or co-assembly of biocompatible interactive units, such as peptides, amino acids, urea, steroids or carbohydrates have recently come into focus due to their non-toxic nature and 'highly specific' on-demand response.[1] Among them, carbohydrate-based hydrogels provide chiral 3D-template in addition to high water affinity and extensive hydrogen bonded networks.[2] Such hydrogels have indeed been used for diverse purposes, such as optical sensing, wound healing, cell encapsulation and sustained drug-release etc.[3] On the other hand, cholera is one of the most acute infectious diseases known to mankind, characterized by profuse watery diarrhoea and vomiting. Cholera Toxin (CT), secreted by Vibrio Cholerae, is responsible for this fatal disease. The crystal structure of CT indicates the presence of a hexameric AB5 type architecture, where the five identical B-subunits specifically bind to the glycolipid gangliosides via galactose units.[4] Thus, galactose-bearing synthetic multivalent systems, such as dendrimers and nanoparticles (Table S1) can show specific interactions with CT.[5] However, till date no attempt has been made to utilize supramolecular hydrogels for bio-sensing of Cholera Toxin. Considering these, we report herein, the design and synthesis of pyrene-based amphiphilic molecules with C4-alkanoyl spacer and disaccharides, such as lactose and maltose as hydrophilic units (Fig. 1a). Interestingly, the conformations, as well as the 3D-arrangements of the sugar hydroxyl groups, showed marked influence on their self-assembly process. The maltose-appended compound (**PyMal**) showed no detectable aggregation in aqueous media, while the lactose analogue (**PyLac**) formed injectable hydrogel under similar conditions (Fig. 1b). Since **PyLac** possesses terminal galactose residue, we anticipated that it might interact with CT. Such binding event can not only alter the fluorescence response of sensor gelator molecule, but also their arrangements in the self-assembled state. Upon encapsulation, the hydrophilic lactose residue would no longer be available for hydrogen bonding. Thus, one could expect that molecular-level interaction with CT might influence the macroscopic property like gel-to-sol transition process.

As mentioned earlier, **PyLac** above a certain concentration [Critical Gelator Concentration (CGC): 1.52 mM], readily formed an opaque gel in pure water. The hydrogel so formed was thermo-reversible as confirmed by the repetitive freeze-thaw cycles (Fig. 1d). Moreover, hydrogel samples remain stable over an extended period without undergoing noticeable decomposition. The gel melting temperature (T_{gel}) of the hydrogel was found to be elevated with the increasing concentration of the gelator indicating the formation of more compact 3-D arrangement (Fig. S1a). Also, the hydrogel rapidly

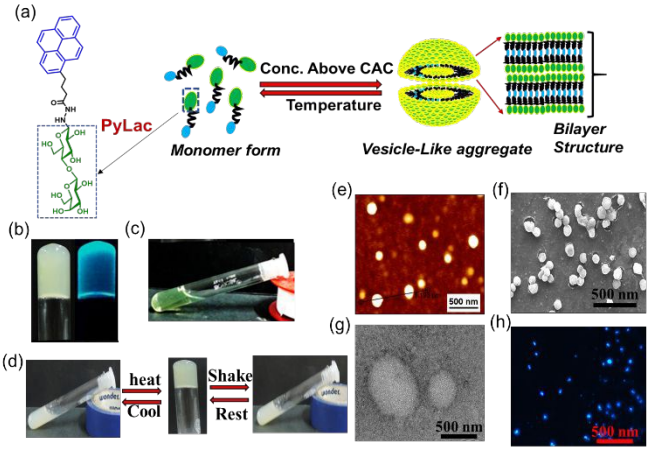

Fig.1. (a) Pictorial representation of **PyLac** amphiphiles in water. Gel picture of **PyLac** (2.5 mM) under (b) daylight and UV lamp (> 365 nm). (c) Sol formation of **PyMal** at high concentration of 10 mM. (d) Gel-to-sol transition in presence of heat/cool and shake/rest. (e) AFM, (f) SEM, (g) TEM images of the solution of **PyLac** (0.09 mM). (h) Fluorescence microscopy images of the solution of **PyLac** (0.18 mM).

[a] *ADepartment of Organic Chemistry, Indian Institute of Science, Bangalore, Karnataka 560012, India*
[b] *School of Applied & Interdisciplinary Sciences, Indian Association for the Cultivation of Science, Kolkata 700032, India*
E-mail: sb@iisc.ac.in, director@iacs.res.in; Tel: +91 (0)33 24734688.; +918022932664

converted to 'sol' under mechanical stress but reverted spontaneously to gel upon resting, thus confirming the thixotropic property of the hydrogel (Fig. 1d). On contrary, even at sufficiently high concentration (~10 mM), **PyMal** does not gelate, rather formed a viscous solution (Fig. 1c). The different behavior of **PyMal** may be attributed to the higher water solubility of the maltose residue compared to that of the lactose, in addition to the configuration, as well as 3-D orientations of the OH groups.

The morphology of the gel was examined using wide range of microscopic imaging. Both SEM (Fig. 1f) and AFM (Fig. 1e) revealed the formation of spherical nanostructures with a diameter of 180 ± 22 nm. On the other hand, TEM indicated the presence of well-defined vesicle-like structures (Fig. 1g). The vesicle-like nanostructures of the hydrogel were also observed under the fluorescence microscopy (Fig. 1h). In order to get the sizes of the vesicle-like aggregates in the solution phase, diluted hydrogel samples were examined by dynamic light scattering (DLS), which indicated the presence of particles with the average hydrodynamic diameter of 303 ± 19 nm (Fig. S1b). Further, the mechanical properties of the hydrogel samples were evaluated via viscoelastic measurements. The oscillatory amplitude sweep experiments (Fig. S2a) revealed that the magnitude of the storage modulus (G') value (viscoelasticity of the hydrogel) increased with increase in gelator concentration. Similarly, the frequency sweep experiment indicated that the viscoelastic behavior of the hydrogel was maintained throughout the frequency range of 1-100 Hz under the applied strain of 0.01% and G' was always greater than that of G" (Fig. 2c). Further, the thixotropic property of the hydrogel was established using a hysteresis loop test. The magnitude of G' dropped from 1751 Pa to 409 Pa when a 30% strain was applied, while the mechanical stiffness of the native hydrogel was restored to almost 97% of the original value within a few secs upon release of the induced strain (Fig.S2b). Such a characteristic of the hydrogel allowed injection of them through a syringe needle of narrow aperture and could be tuned into various alphabetical shapes (Fig. 2b).[6]

In order to examine the mode of self-assembly, the FT-IR spectrum of solid **PyLac** was compared with that of the dried gel (Fig. 2a). The stretching frequencies of N-H and O-H groups in solid **PyLac** were observed at 3414 and 3298 cm^{-1} respectively, which shifted to 3391 and 3290 cm^{-1} in case of the dried hydrogel. This suggests the presence of H-bonding interaction during the gelation. IR spectra also showed the shifting of C=O (amide group) from 1650 cm^{-1} to 1642 cm^{-1}, confirming the participation of hydrazide units in intermolecular H-bonding. In addition, the presence of the pyrene unit allowed us investigation of the assembling nature of the gelator molecules by conventional spectrophotometric methods. Variable concentration UV/Vis spectra of **PyLac** showed the presence of well-resolved vibronic peaks of 'monomeric' pyrene species at relatively low concentrations, whereas, on increasing concentration (> 0.05 mM), one could witness broad spectrum with residual absorbance at a longer

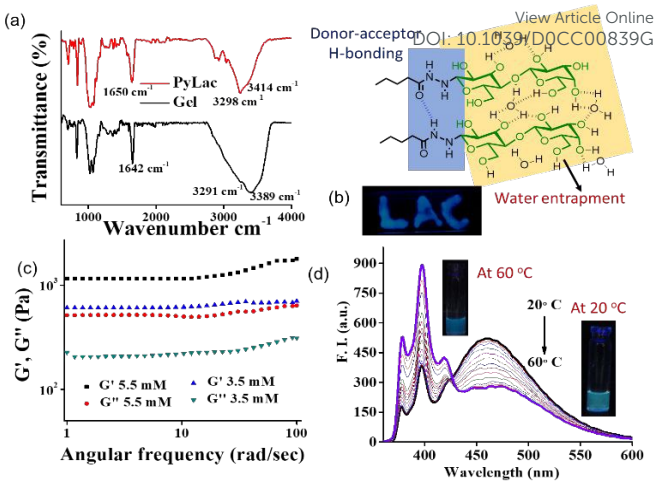

Fig.2 (a) FT-IR spectra of solid and dried hydrogel of **PyLac**. (b) Injectability property of **PyLac** hydrogel. (c) Concentration dependent oscillatory frequency sweep rheology data of **PyLac**. (d) Variable temperature fluorescence of **PyLac** (0.80 mM) solution.

wavelength range, suggesting the formation of larger aggregates (Fig. S3).[7] Similarly, the concentration-dependent emission spectra (Fig. S4a) revealed the presence of two distinct bands at 378 and 396 nm at lower concentrations, resembling the vibronic bands of the 'monomeric' pyrene moiety with critical aggregation concentration (CAC) of 0.02 mM (Fig. S4b). However, formation of broad emission band at 470 nm was observed at high gelator concentration. This red-shifted emission band may be attributed to a combination of aggregation, π-π stacking and H-bonding interactions. The relatively high average decay constant (τ_{av} = 1.27) observed at 470 nm band further confirmed our proposition.[8] Variable temperature emission studies show gradual diminution of the fluorescence intensity at 470 nm, suggesting heat-mediated 'breaking' of the 'slipped' π-π stacking structures (Fig. 2d).

The supramolecular chirality of **PyLac** hydrogel was established by circular dichroism (CD) studies, where the presence of a positive bisignated signal was observed at high concentration, indicating that the chiral information of the sugar unit is transferred to the pyrenyl moiety in the self-assembled state, leading to the formation of P-helical (right-handed helical) aggregates (Fig. S5a). Further, the unperturbed positive cotton signal during variable-concentration studies suggests that concentration of monomer units have no affect on the nature of the chiral assembly. Moreover, intensity of the CD signal was found to be quenched at elevated temperature and almost no detectable CD signal was observed beyond 65 °C (Fig.3a, S5b) indicating heat-mediated disassembly of the ordered arrangement. To understand the packing of molecules in the self-assembled state, the powder X-Ray diffraction (p-XRD) of freeze-dried gel samples were performed, which showed the presence of Bragg reflection peaks at 2θ = 3.29°, 8.69°, 12.84° indicating the corresponding d-spacings at 2.06, 1.02, 0.69 nm respectively (Fig. 3b). The reciprocal ratio of these reflection peaks was found to be 1:1/2:1/3 suggesting lamellar arrangements of gelator molecules with a repetitive distance of 2.06 nm. XRD studies

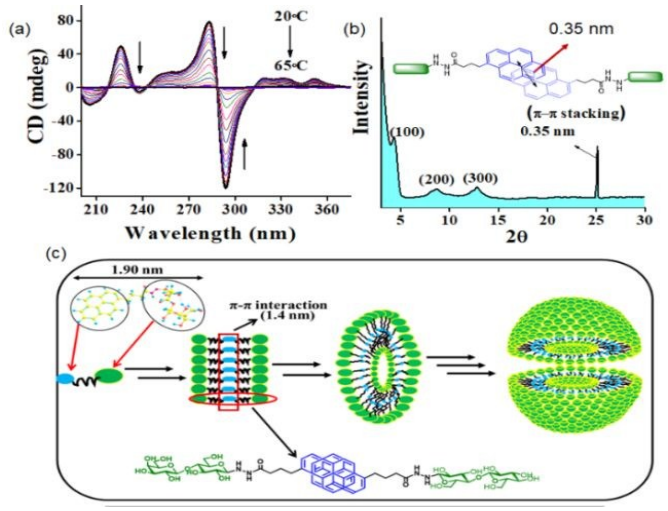

Fig. 2 (a) Variable temperature CD spectra of **PyLac** (0.20 mM) solution. (b) p-XRD spectra of freeze-dried hydrogel of **PyLac**. (c) Proposed nano-structural model for the formation of **PyLac** hydrogel.

further revealed the presence of reflection peaks at 25.1° with a d-spacing value of 0.35 nm and this is presumably due to the characteristic π-π interaction among the pyrenyl units. On the other hand, the molecular length, calculated from energy optimized structure, was found to be 1.90 nm (Fig. 3c).

Thus, from the above shreds of evidences, one can speculate the arrangement of the **PyLac** molecules in the 3-D hydrogel network. Since the molecular length obtained from the computational studies is found to be shorter than that of the XRD studies, one can assume significant interdigitation of the pyrene residues in hydrogel.[9] As expected, due to hydrophobic nature, the polyaromatic pyrenyl units stay away from the bulk water while lactose moieties direct towards water owing to the presence of free -OH units. The formation of extensive H-bonding network via both hydrazone (donor-acceptor type) and lactose units is feasible.[10] Most importantly, at high concentration (above CGC value), these molecular level interactions help propagation of the self-assemblies into three-dimensional structures, which ultimately leads to the formation of vesicle-like morphology (Fig.3c).

Since **PyLac** amphiphiles possess galactose units at the terminal position, the current system was employed for optical sensing of CT. For all subsequent spectroscopic studies, we have used **PyLac** concentration as 0.8 mM, which is lower than its CGC value but higher than CAC. This suggests that **PyLac** exists essentially in the aggregated state at this concentration in water. As expected, **PyLac** showed cyan colored fluorescence at this condition with a broad emission band at ~470 nm, along with sharp peaks at 380-440 nm region. Addition of CT to the aqueous solution of **PyLac** resulted in a ~5.3-fold quenching of the emission intensity at 470 nm band with ~14 nm blue-shift in the emission maximum (Fig. 4a). Thus, the color of the solution turned from cyan to blue in the presence of CT. The CT-triggered 'dissociation' of the performed molecular assembly might be the probable reason for this fluorescence quenching, while blue-shift indicates hetero-assembly formation between gelator molecules and multivalent CT protein. Moreover, titration studies (Fig.4a) indicate that the present system is quite sensitive in nature and could detect CT at as low as 0.4 μM in aqueous media. A closer look at the emission profile showed an increase in the I_1/I_3 value (I_1 = intensity at 377 nm band, I_3 = intensity at 396 nm band) with a rising concentration of CT. The smaller I_1/I_3 value at lower concentration of CT indicates hydrophobic environment around the pyrene moiety of the hydrogelator due to its aggregated form in the native state, while the larger I_1/I_3 value at higher CT concentration suggests an increase in the local polarity during the formation of hydrogelator-CT assembly (Fig. S6a).[11] To verify the formation of such hetero-aggregates in the presence of CT, we repeated the titration of **PyLac** with CT (Fig.4b) at a lower concentration of the hydrogelator (5 μM). At this concentration, no distinguishable emission peak was observed at 470 nm. However, upon titration with CT, emission intensity at 455 nm band enhanced with concomitant quenching at both 377 and 396 nm bands. Thus, at low concentration of **PyLac,** ratiometric probing of CT is possible. Moreover, the UV-Visible spectra of a **PyLac** (5 μM) in the presence of CT (8 μM) showed a loss of fine-structured profile with an increase in the absorbance value at the higher wavelength region (Fig. S6b).

Both observations reinforce the idea of toxin-mediated hetero-assembly formation. Importantly, the specificity of **PyLac** towards CT was retained even in the presence of a large number of competitive analytes (Fig. 4c). As expected, a drastic increase in hydrodynamic diameter from ~50 ± 10 nm to 440 ± 25 nm was observed when **PyLac** at 5 μM concentration was treated with CT (Fig. S7a-b). Similarly, time-dependent emission studies of **PyLac** showed multi-exponential decay (at 470 nm) with a large average time-constant (τ_{av} = 1.3) in the presence of CT (Fig. 4d). This enhanced average lifetime of **PyLac** can be correlated with the slower dynamics of the dye molecules upon binding with CT.[12]The transmission electron microscopic images also show aggregation of the **PyLac** molecules in the presence of CT (Fig.S7c-d). Further, to prove the importance of the terminal

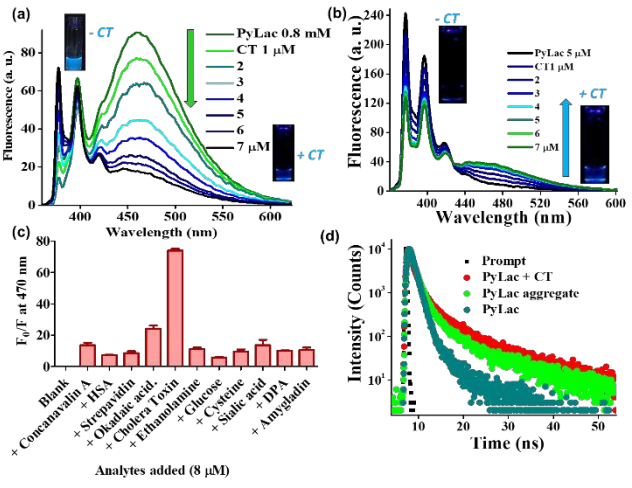

Fig. 3 Titration of (a) **PyLac** (0.8 mM), (b) **PyLac** 5μM with increasing CT concentration. (c) Selectivity studies for the interaction **PyLac** (0.8 mM) with different analyte. (d) Fluorescence Decay profile of **PyLac** in presence and absence of CT.

View Article Online
DOI: 10.1039/D0CC00830C

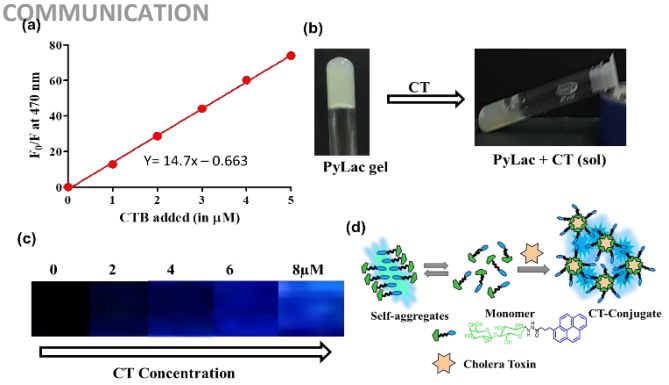

Fig. 4 (a) Linear change in the emission intensity of **PyLac** (5 μM, λ_{ex} = 345 nm) with increasing CT (0-8 μM) in the presence of different analyte present in stool samples. (b) Gel-to-sol transition in the presence of CT (0.6 mM). (c) Images captured (UV lamp > 365 nm after addition of CT onto pre-coated TLC plate of **PyLac** hydrogel. (d) Pictorial representation for the interaction of **PyLac** with CT.

galactose unit, the interaction of CT was also monitored in the presence of **PyMal** compound (Fig. S7e). In spite of high structural similarity, this compound showed no interaction with CT, indicating the indispensable role of the terminal galactose unit in the sensing process.

Further, **PyLac** was utilized for detecting CT in the presence of various ionic analytes, commonly present in the watery stool samples (diarrhoea).[13] Since, no interaction was seen from any of these analytes, it is anticipated that **PyLac** can even be used for clinical diagnosis (Fig. S8). Further, a dose-dependent linear change in the emission intensity was observed with CT (0-5 μM) (Fig.5a). Also, the present system was engaged in the estimation of CT in different types of natural water samples. For this, water samples were collected from different places were incubated with various amounts of CT (0-4 μM) prior to spectral analysis. Recovery analysis indicates that in most cases the proportional error was less than 5%, which indeed is an exciting observation (Fig.S9).

The fact that CT interacts with **PyLac** at molecular level, intrigued us to check its effect on preformed supramolecular assembly. Interestingly, the addition of CT (0.6 mM) in sub-stoichiometric amount into a preformed gel sample (3 mM) immediately induced a gel-to-sol transition (Fig. 5b). The binding of CT to galactose units possibly disrupted the H-bonding network, leading to the breakdown of self-assembled structure and the consequent induction into sols (Fig. 5d). Further, to check the relevance of both the pyrene and lactose units in CT sensing, two more hydrogel systems were examined. Though in this case, both maltose (**1**) and lactose (**2**) appended probes form hydrogel, selective gel to sol transition was observed only in case of **1**. Also, such observations ruled out the direct involvement of pyrene in the sensing process (Table S10). To employ the sensory systems even in remote areas, we developed low-cost paper strips for rapid detection of Cholera Toxin. The **PyLac** (0.8 mM) gel coated paper strips showed quenching of cyan fluorescence in the presence of CT. Remarkably, even on such paper strips, we could see dose-dependent changes in the emission intensity (Fig. 5c).[14]

In conclusion, we present here a thermoreversible injectable hydrogel based on a pyrene-disaccharide (**PyLac**) in which both configurations, as well as 3-D orientations of the OH groups of the sugar moiety showed profound effect in controlling the self-assembly process. The viscoelastic measurement indicates thixotropic nature of the gel, whereas, morphological analysis showed formation of vesicle-like nanostructures. Importantly this lactose-bearing pyrenyl system exhibited color changing response (ratiometric biosensing) in the presence of cholera toxin (CT). Addition of CT induced dissociation of the preformed self-assembled structure of **PyLac** by concurrent formation of a 'more stable' hetero-aggregate, further led to gel-to-sol transition.

Conflicts of interest

There are no conflicts to declare.

Notes and references

1 (a) J. Mayr, C. Saldias and D. D. Diaz, *Chem. Soc. Rev.*, 2018, **47**, 1484-1515; (b) S. Akama, T. Makia and M. Yamanaka *Chem. Commun.*, 2018, **54**, 8814-8817. (c) B. Pramanik, N. Singha and D. Das, *ACS Appl. Polym. Mater.* 2019, **1**, 833–843.

2 S. Datta and S. Bhattacharya, *Chem. Soc. Rev.*, 2015, **44**, 5596-5637.(b) S. Himmelein, V. Lewe, M. C. A. Stuart and B. J. Ravoo, *Chem. Sci.*, 2014, **5**, 1054-1058; (c) S. Bhattacharya and S. N. G. Acharya, *Chem. Mater.*, 1999, **11**, 3504-3511. (d) S. Bhattacharya and S. N. G. Acharya, *Langmuir*, 2000, **16**, 87-97.

3 (a)Q. Chen, Y. Lv, D. Zhang, G. Zhang, C. Liu and D. Zhu, *Langmuir*, 2010, **26**, 3165-3168; (b) X. Li, Y. Kuang, J. Shi, Y. Gao, H. C. Lin and B. Xu, *J. Am. Chem. Soc.* 2011, **133**, 17513-17518; (c) S. Lu, C. Gao, X. Xu, X. Bai, H. Duan, N. Gao, C. Feng, Y. Xiong and M. Liu, *ACS Appl. Mater. Interfaces*, 2015, **7**, 23, 13029-13037; (d) H. Xu, L. Zhang and J. Cai, *ACS Appl. Bio Mater.*, 2019, **2**, 196-204.

4 (a) C. L. Schofield, R. A. Field and D. A. Russell, *Anal. Chem.*, 2007, **79**, 1356-1361; (b) K. S. Ahn, K. R. Lim, D. Jeong, B. Y. Lee, K. S. Kim and W. Y. Lee, *Microchem. J.*, 2016, **124**, 9-14; (c) G. Ma and Q. Cheng, *Langmuir*, 2006, **22**, 6743-6745.

5 (a) X. M. Hu, Q. Chen, J. X. Wang, Q. Y. Cheng, C. G. Yan, J. Cao, Y. J. He and J. B. H. Han, *Chem. Asian J.*, 2011, **6**, 2376-2381;(b) S. A. Khan, J. A. DeGrasse, B. J. Yakes, and T. R. Croley, *Anal. Chim. Acta*, 2015, **892**, 167-174.

6 S. Bhattacharjee and S. Bhattacharya, *J. Mater. Chem. A*, 2014, **2**, 17889-17898.

7 M. M. Islam, Z. Hu, Q. Wang, C. Redshaw and X. Feng, Mater. Chem. Front., 2019, 3, 762-781.

8 A. Gulyani, N. Dey and S. Bhattacharya, *Chem. Eur. J.,* 2018, **24**, 2643-2652.

9 S. Bhattacharjee, B. Maiti and S. Bhattacharya, *Nanoscale,* 2016, **8**, 11224-11233.

10 H. Qian and I. Aprahamian, *Chem. Commun.,* 2015, **51**, 11158-11161.

11 D. Kim, R. Amos, M. Gauthier and J. Duhamel, *Langmuir* 2018, **34**, 8611-8621.

12 N. Dey, D. Biswakarma, A. Bajpai, J. N. Moorthy and S. Bhattacharya, *ChemPhysChem*, 2019, **20**, 881-888.

13 R. L. Guerrant, B. A. Carneiro-Filho and R. A. Dillingham, *Clin. Infect. Dis.,* 2003, **37**, 398–405.

14 (a) N. Dey, D. Biswakarma, S. Bhattacharya, *ACS Sustain. Chem. Eng.*, 2018, **7**, 569-577. (b) N. Dey, S. Jha, S. Bhattacharya, *Analyst*, 2018, **143**, 528-535.